Received November 1999
Revised May 2000
Accepted May 2000

Natural convection in enclosures with localized heating from below and symmetrical cooling from sides

Orhan Aydin and Wen-Jei Yang
Department of Mechanical Engineering and Applied Mechanics, University of Michigan, Ann Arbor, Michigan, USA

Keywords *Natural convection, Enclosures*

Abstract *Natural convection of air in a two-dimensional, rectangular enclosure with localized heating from below and symmetrical cooling from the sides has been numerically investigated. Localized heating is simulated by a centrally located heat source on the bottom wall, and four different values of the dimensionless heat source length, 1/5, 2/5, 3/5 and 4/5 are considered. Solutions are obtained for Rayleigh number values from 10^3 to 10^6. Local results are presented in the form of streamline and isotherm plots as well as the variation of local Nusselt number on the heated wall. Finally, the average Nusselt number at the heated part of the lower wall,* $\overline{\mathrm{Nu}}$*, was shown to increase with an increase the Rayleigh number,* Ra*, or of the nondimensional heat source thickness,* ϵ*.*

Nomenclature

g = gravitational acceleration, m/s^2
Gr = Grashof number, dimensionless
H = height of the enclosure, m
l = length of the heat source, m
L = length of the enclosure, m
n = coordinate in normal direction
Nu = Nusselt number, dimensionless
Pr = Prandtl number, dimensionless
Ra = Rayleigh number, dimensionless
T = temperature, K
t = time, s
u = velocity component in x-direction, m/s
U = nondimensional velocity component in x-direction
v = velocity component in y-direction, m/s
V = nondimensional velocity component in y-direction
x, y = coordinates defined in Figure 1
X,Y = nondimensional coordinates

Greek symbols
α = thermal diffusivity, m^2/s
β = thermal expansion coefficient, 1/K
ζ = vorticity, 1/s
θ = nondimensional temperature
ξ = nondimensional vorticity
τ = nondimensional time
ψ = stream function, m^2/s
Ψ = nondimensional stream function
ϵ = nondimensional length of the heat source
Φ = generalized nondimensional variable

Subscripts
C = cold wall
H = hot wall
i, j = coordinate indices
wall = at wall
x = in x-direction
y = in y-direction

Introduction

The study of natural convection in enclosures provides a useful description of the confined fluids in many practical situations. Most of the previous studies

International Journal of Numerical Methods for Heat & Fluid Flow, Vol. 10 No. 5, 2000, pp. 518-529.

have addressed natural convection in enclosures due to either a horizontally or vertically imposed temperature difference. However, departures from this basic situation are often encountered in such fields as the electronics cooling. The cooling of electronic components is essential for their reliable operation. Natural convection cooling has been widely used because of its simplicity, low cost and reliability (Incropera, 1988; Peterson and Ortega, 1990; Kim and Lee, 1996).

Torrance *et al.* (1969) experimentally and Torrance and Rockett (1969) numerically studied the convection of air in a vertical cylindrical enclosure, induced by a small hot spot centrally located on the floor. Solutions were obtained for Grashof numbers from 4×10^4 to 4×10^{10}. The theoretical results were found to be in an excellent agreement with the experimental ones in the laminar region. Chu *et al.* (1976) studied, both theoretically and experimentally, the effect of the size and location of an isothermal, horizontal strip in an otherwise insulated vertical surface of a rectangular channel. For a similar cavity, Turner and Flack (1980) made an experimental study. The natural convection in an inclined box with the half of the lower surface heated and the other half insulated was investigated experimentally and numerically by Chao *et al.* (1983). The effects of elevation of the heated and insulated segments were investigated, as well as of inclination about the longer dimension. An experimental investigation was conducted by Kamotani *et al.* (1983) to study natural convection heat trasnfer in a water layer with localized heating from below. The flows were driven by maintaining a small circular heat source, at a uniform temperature. The flow structures and temperature fields were investigated in detail for various aspect ratios (depth/width) and Grashof numbers Gr. Steady natural convection in a square, water-filled enclosure heated from below and cooled on one vertical side is studied analytically and numerically by November and Nansteel (1987). Keyhani *et al.* (1988) investigated, both numerically and experimentally, natural convection in a vertical cavity with one isothermal vertical cold wall and three alternatively adiabatic and flush-heated sections of equal height on the opposite wall. A numerical investigation of natural convection of air in square cavities with half-active and half-insulated vertical wall was made by Valencia and Frederick (1989). An experimental and numerical study was made by Chu and Hichox (1990) for natural convection in an enclosure with localized heating from below in order to simulate the convective transport in a magma chamber. The large viscosity variation characteristics of magma convection was simulated by using corn syrup as the working fluid. Hasnaoui *et al.* (1992) numerically investigated natural convection in an enclosure with localized heating from below. The upper surface was cooled at a constant temperature and a portion of the bottom surface was isothermally heated while the rest of the bottom surface and vertical walls were adiabatic. The existence of multiple steady-state solutions and the oscillatory behavior for a given set of the governing parameters were demonstrated. Ganzorolli and Milanez (1995) numerically

analyzed steady natural convection in an enclosure heated from below and symmetrically cooled from the sides. The effects of the Rayleigh number, the Prandtl number and aspect ratio on the flow and energy transport were determined. Ramos and Milanez (1998) performed an experimental and numerical analysis for natural convection flow caused by heat sources dissipating energy at a constant rate simulating electronic components mounted at the bottom surface of a cavity symmetrically cooled from the sides and insulated at the top.

In the present study, natural convection in a square enclosure with localized heating from below and symmetrical cooling from the sides is considered. As it appears from the existing literature, this study is the first attempt at studying the natural convection phenomenon in an enclosure under the above mentioned thermal conditions. Symmetrical cooling from the sides is expected to be an efficient cooling option, while partial heating at the lower surface simulates the electronic components such as chips. Since natural convection flows in enclosures arise in many engineering processes, the results to be obtained here may be applicable to other fields of interest. The effects of the Rayleigh number and the nondimensional isothermal heat source length on the fluid flow and heat transfer are determined. For $\epsilon = 0$, which means that the whole part of the lower wall is heated, the boundary conditions applied here are identical to those considered by Ganzorolli and Milanez (1995).

Analysis

Consider the motion of a viscous fluid within a square enclosure with equal length and height, $L = H$, which is depicted in Figure 1. The size of the

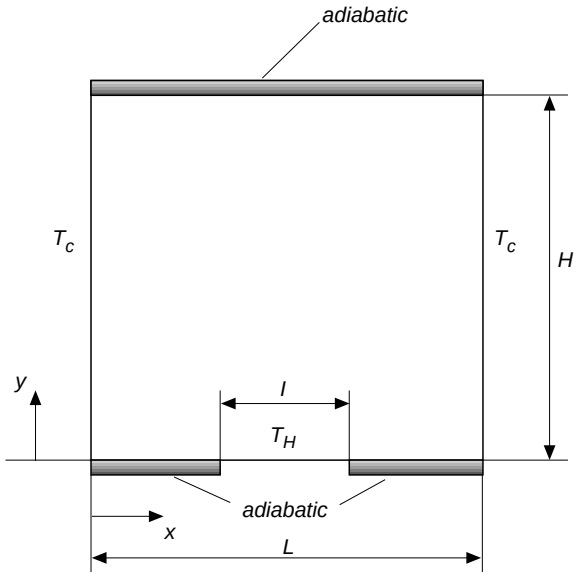

Figure 1.
Geometry and boundary conditions of the problem

enclosure in z-direction is assumed to be infinitely long. The lower wall has a centrally located heat source which is assumed to be isothermally heated at a constant temperature T_H. The sidewalls are isothermally cooled at a constant temperature T_C, while the bottom surface, except for the heated section, and the upper wall are considered to be adiabatic.

Mathematical formulation

The nondimensional set of the governing equations (stream function, vorticity and energy equations) for a two-dimensional, incompressible laminar flow with constant fluid properties are given as (Aydın *et al.*, 1999a)

$$\frac{\partial^2 \Psi}{\partial X^2} + \frac{\partial^2 \Psi}{\partial Y^2} = -\xi \tag{1}$$

$$\frac{\partial \xi}{\partial \tau} + U\frac{\partial \xi}{\partial X} + V\frac{\partial \xi}{\partial Y} = Pr\left(\frac{\partial \xi^2}{\partial X^2} + \frac{\partial \xi^2}{\partial Y^2}\right) + RaPr\frac{\partial \theta}{\partial X} \tag{2}$$

$$\frac{\partial \theta}{\partial \tau} + U\frac{\partial \theta}{\partial X} + V\frac{\partial \theta}{\partial Y} = \frac{\partial^2 \theta}{\partial X^2} + \frac{\partial^2 \theta}{\partial Y^2} \tag{3}$$

where the nondimensional parameters including stream function and vorticity are defined in the following forms

$$X = \frac{x}{H} \quad Y = \frac{y}{H} \quad \theta = \frac{T - T_C}{T_H - T_C} \quad \tau = \frac{\alpha t}{H^2} \quad U = \frac{u}{\alpha/H} \quad V = \frac{v}{\alpha/H} \tag{4}$$

$$U = \frac{\partial \Psi}{\partial Y} \quad V = -\frac{\partial \Psi}{\partial X} \quad \xi = \frac{\partial V}{\partial X} - \frac{\partial U}{\partial Y} \tag{5}$$

Appearing in equation (3), $Pr = \nu/\alpha$ is the Prandtl number and $Ra = g\beta H^3(T_H - T_C)/\nu\alpha$ is the Rayleigh number.

Boundary conditions

Through the introduction of the nondimensional parameters into the physical boundary conditions illustrated in Figure 1, the following nondimensional boundary conditions are obtained:

$$\theta = 0 \quad U = V = 0 \quad at \quad X = 0, 1, \quad 0 < Y < 1 \tag{6}$$

$$\theta = 1 \quad U = V = 0 \quad at \quad Y = 0, \quad \frac{1-\epsilon}{2} \leq X \leq \frac{1+\epsilon}{2} \tag{7}$$

$$\frac{\partial \theta}{\partial Y} = 0 \quad U = V = 0 \quad at \quad Y = 0, \quad 0 < X < \frac{1-\epsilon}{2}, \frac{1+\epsilon}{2} < X < 1 \tag{8}$$

$$\frac{\partial \theta}{\partial Y} = 0 \quad U = V = 0 \quad at \quad Y = 1, \quad 0 < X < 1 \tag{9}$$

For stream function, the boundary condition for entire surface of the enclosure is taken to be

$$\Psi = 0 \tag{10}$$

which implies that there is no mass transfer through the walls of the enclosure and that the boundaries themselves form one of the stream lines.

In general, the value of the vorticity on a solid boundary is deduced from Taylor series expansion of the stream function Ψ around the solid point and can be expressed mathematically as

$$\xi_{wall} = -\frac{\partial^2 \Psi}{\partial n^2} \tag{11}$$

where ξ_{wall} is the value of the vorticity at wall and n is the outward drawn normal of the surface. In numerical calculations, the values of vorticity at corners are taken as averages of the values of vorticity at two neighboring nodes (Aydın *et al.*, 1999a).

The average Nusselt numbers, $\overline{Nu}$ for the heated portion of the lower wall is given by

$$\overline{Nu} = \int_{\frac{1-\epsilon}{2}}^{\frac{1+\epsilon}{2}} Nu(X) dX \tag{12}$$

where $Nu(X)$ is the local Nusselt number and is given by

$$Nu(X) = \left[-\frac{\partial \theta}{\partial Y} \right]_{Y=0} \tag{13}$$

Numerical procedure

The governing equations along with the boundary conditions are solved numerically, employing finite-difference techniques. The vorticity transport and energy equations are solved using the alternating direction implicit method of Peaceman and Rachford (Roache, 1982), and the stream function equation is solved by SOR (successive over-relaxation) method (Patankar, 1980). The over-relaxation parameter is chosen to be 1.8 for stream function solutions. In order to avoid divergence in the solution of vorticity equation an under-relaxation parameter of 0.5 is employed. The buoyancy and diffusive terms are discretized by using central differencing while the use of hybrid differencing is preferred for convective terms for numerical stability. Starting from arbitrarily specified initial values of variables, the discretized transient equations are then solved by marching in time until an asymptotic steady-state solution is reached.

Convergence of iteration for stream function solution is obtained at each time step. The following criterion is employed to check for steady-state solution

$$\sum_{i,j} \left| \Phi_{i,j}^{n+1} - \Phi_{i,j}^{n} \right| \leq ERMAX \tag{14}$$

where Φ stands for Ψ, ξ, or θ; n refers to time and i and j refer to space coordinates. The value of ERMAX is chosen as 10^{-5}. The time step used in the computations is varied between 0.0001 and 0.001, depending on Rayleigh number and mesh size.

A non-uniform mesh structure is employed, which is constructed using finer grid spacing near the walls and the mixed boundary points for each case. The mesh structure is changed for each ϵ because of the shifted position of the mixed boundary points. For each case, a mesh refinement study is conducted and finally the mesh structure on which finer mesh refinement does not have a significant effect on the results is chosen and used for simulations. As an example, for $\epsilon = 1/5$ at $Ra = 10^6$, it is observed that increasing the mesh size from 51×51 to 81×81 resulted in the changes of Ψ_{max} and $\overline{Nu}$ by less than 1 percent. Therefore, 51×51 mesh size is approved to be sufficient to resolve the velocity and temperature fields for the related case.

The validity of the computer code developed has been already verified for the problem of natural convection in a square cavity having differentially heated vertical walls and the problem of laminar natural convection in inclined air layers heated from above (Aydın *et al.*, 1999a; 1999b).

Results and discussion

Flow fields, temperature fields, and heat transfer rates for various values of the Rayleigh number and the nondimensional size of the isothermal heat sources are examined in this section. In order to simulate air cooling of electronic components air is chosen as the working fluid ($Pr = 0.71$).

The main characteristics of the natural convection flow and energy transport in an enclosure including a centrally located isothermal heat source are shown in Figure 2-5. Flow and temperature fields are shown in terms of streamlines and isotherms, respectively. For each case, 20 equally spaced contours have been used to define the corresponding structure. These figures show the effect of changing Rayleigh number for $10^3 \leq Ra \leq 10^6$ and the effect of changing the dimensionless length of the heat source for $\epsilon = 1/5$, 2/5, 3/5 and 4/5. Owing to the symmetrical boundary conditions on the vertical walls, the flow and temperature fields are symmetrical about the mid-length of the enclosure. The symmetrical boundary conditions in the vertical direction result in a pair of counter-rotating cells in the left and right halves of the enclosure for all the parametric values considered. Owing to the symmetry, the flows in the left and right halves of the enclosure are identical except for the sense of rotation. Each cell ascends through the symmetry axis, then faces the upper

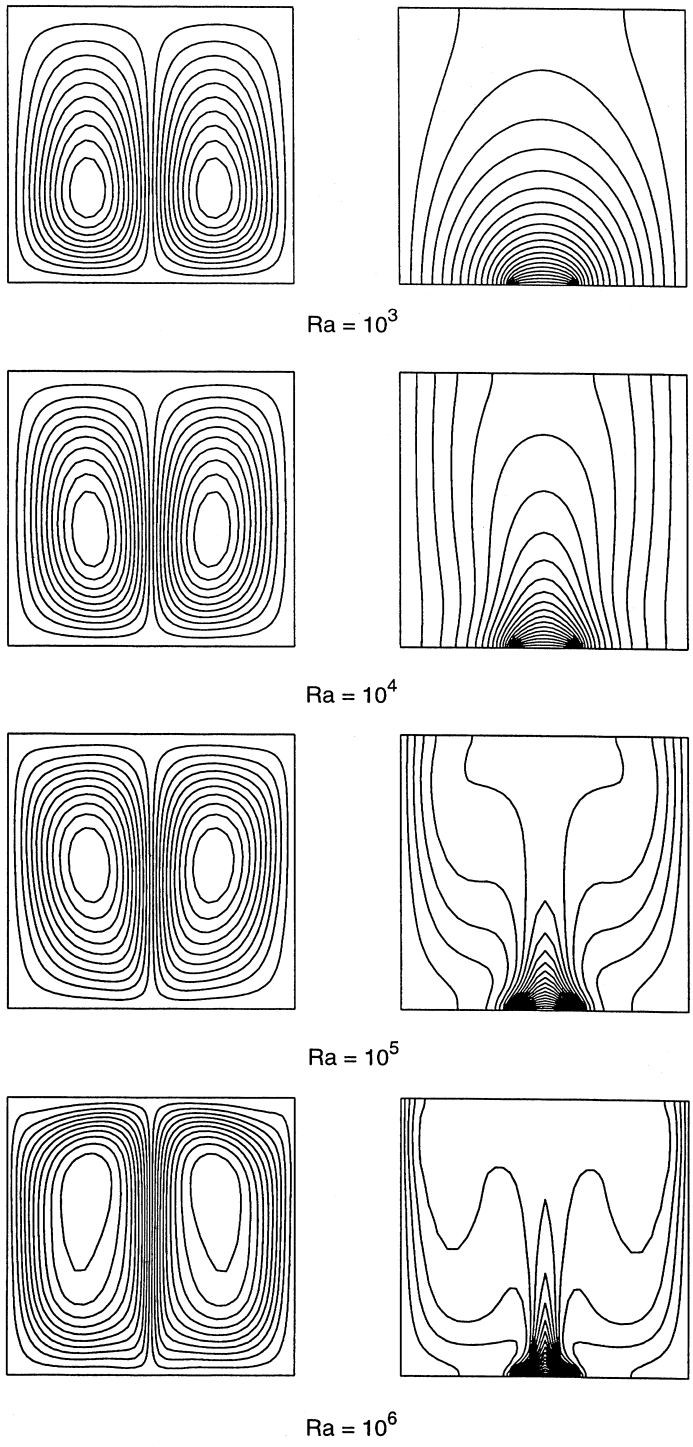

Figure 2.
Streamlines and isotherms for $\epsilon = 1/5$

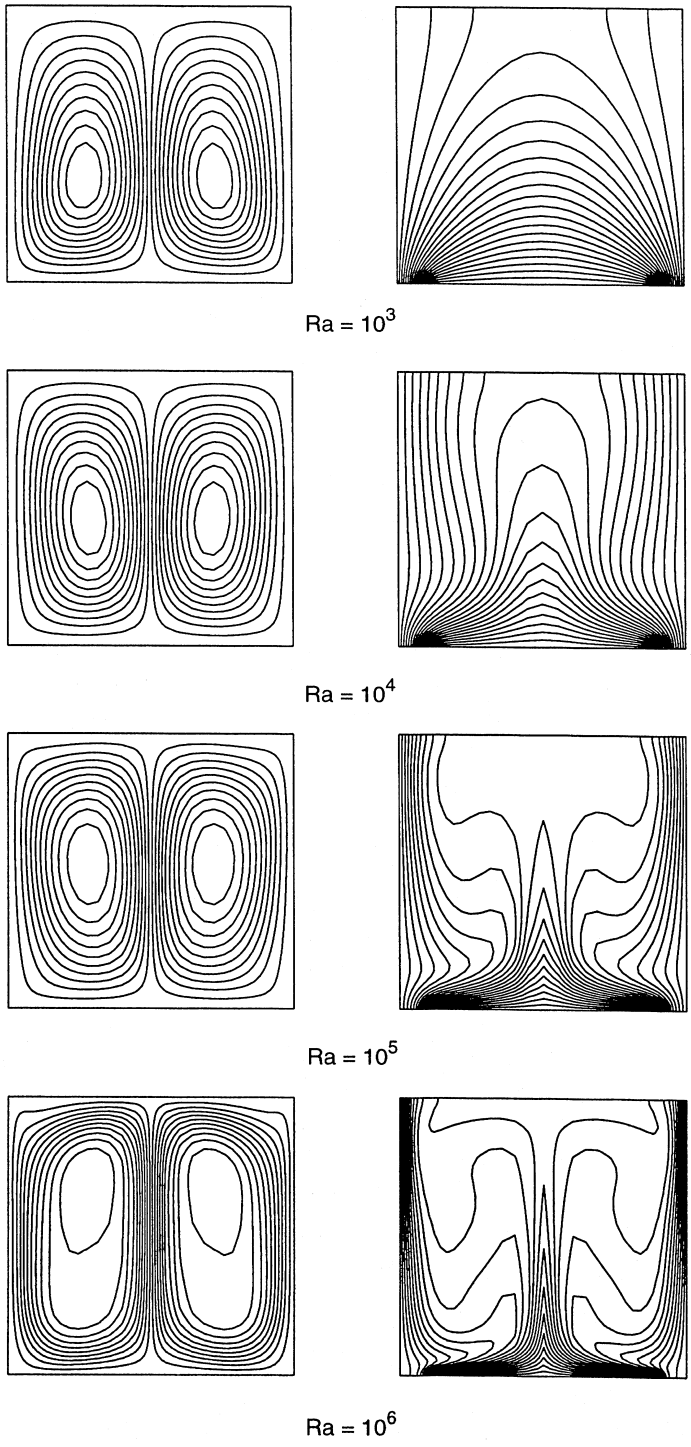

Figure 3.
Streamlines and isotherms for $\epsilon = 4/5$

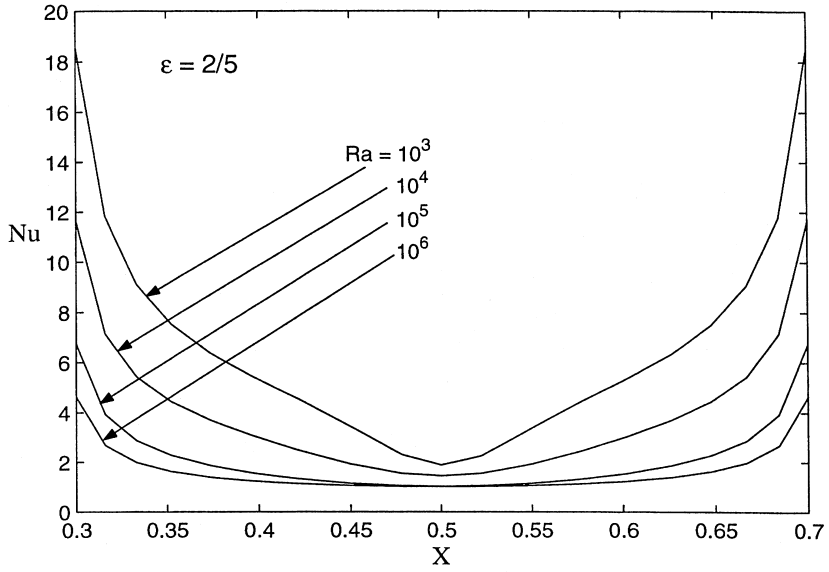

Figure 4.
Variation of the local Nusselt number Nu at the heated wall for various Rayleigh numbers at $\epsilon = 2/5$

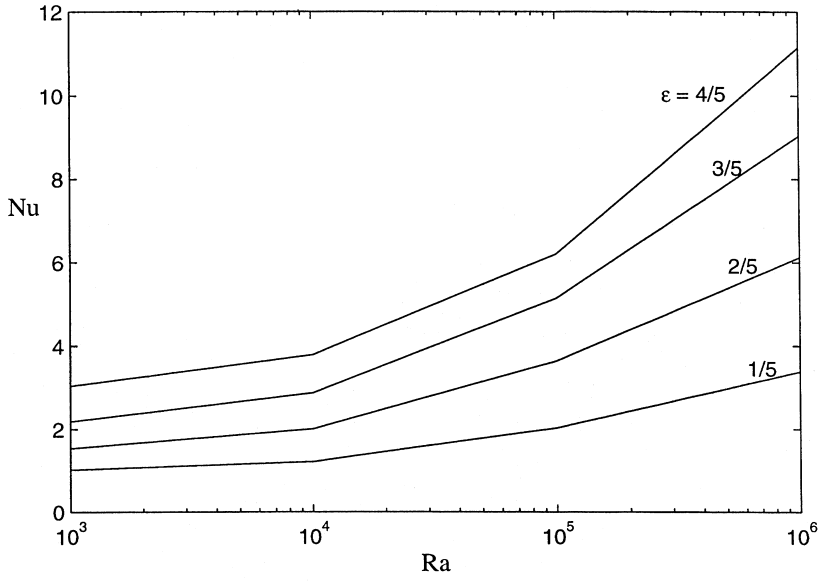

Figure 5.
Variation of the average Nusselt number $\overline{Nu}$ at the heated wall with the Rayleigh number for various nondimensional heat source lengths, ϵ

adiabatic wall through which it moves horizontally toward the corresponding cold wall and finally it descends along the corresponding cold wall under the effect of cooling.

Figure 2 illustrates the streamline and isotherm patterns obtained for $\epsilon = 1/5$. For $Ra = 10^3$, the circulation inside the enclosure is so weak that the viscous

forces are dominant over the buoyancy force. As it can be seen from the figure, isotherms deviate slightly from a diagonally symmetric structure, which is the conduction solution ($Ra = 0$). This leads the conduction to be dominant heat transfer mechanism inside the enclosure. With increasing Rayleigh number, the intensity of the recirculation inside the enclosure increases and the cores of the cells move upward. At $Ra = 10^4$, isotherms deviates from the diagonally symmetric structure and conduction and advection modes of heat transfer are in a comparable level. Beyond $Ra = 10^4$, the distortion of the isotherms increases more and more and the advection takes the revenge, becoming the dominant mode of heat transfer. At $Ra = 10^5$, the formation of thermal boundary layers can be observed due to increased recirculation intensity. At $Ra = 10^6$, the thermal boundary layers become thinner causing increased energy transport. In addition, isotherms become stratified and the degree of stratification increases with increasing Ra. Streamlines and isotherms for $\epsilon = 4/5$ at different Rayleigh numbers are seen in Figure 3. The flow fields are nearly identical to those of $\epsilon = 1/5$ for each Rayleigh number. However, the isotherms are effected by the increasing ϵ, as expected. Since the heated part of lower surface is larger than that of $\epsilon = 1/5$, the heating effect at this case is much more sensible for the same values of Rayleigh numbers. For a fixed Ra, with increasing ϵ, the flow field remains almost the same, while the temperature fields changes becoming more stratified for larger values of Ra.

Owing to the symmetry in the temperature field, heat transfer is symmetrical with respect to mid-length ($x = L/2$), hence $Nu\left(x = \frac{L-l}{2}\right) = Nu\left(x = \frac{L+l}{2}\right)$. As an illustrative example, Figure 4 shows the variation of Nu along the heated part of the lower wall for $\epsilon = 2/5$ for various Rayleigh numbers. The higher Ra means more heat input, and as a result, more heat is added to the fluid to intensify the fluid convection. The intensified fluid convection, in turn, enables more heat to be received by the fluid pack through convective heat transfer. The most striking feature of this figure is the minimum at heat transfer in $X = 1/2$. This minimum originates from the symmetrical boundary conditions applied in the vertical direction. The dual-cell structure prohibits direct convective transfer between these two cells. Each cell behaves like an insulator preventing the fluid pack from coming into contact with opposite cold wall.

Plots of the average Nusselt number on the heated part of the lower wall as a function of Ra and ϵ are shown in Figure 5. For a fixed ϵ, increasing Ra enhances convection. In addition, increasing ϵ for a fixed Ra results in an increase at $\overline{Nu}$, which is more significant for high Ra values. These results can be clearly explained under the views of the isotherms given in Figure 2 and 3.

Conclusion

In this investigation, the results of a numerical study of buoyancy-induced flow and heat transfer in a two-dimensional square enclosure with localized heating from below and symmetrical cooling from the sides are presented. The main

parameters of interest are Rayleigh number and the dimensionless heat source length. The flow and temperature fields are symmetrical about the mid-length of the enclosure due to the symmetry of the boundary conditions in the vertical direction. For small Ra, the heat transfer is dominated by conduction across the fluid layer, while for high Ra the process is primarily one of convection, and the effect of conduction vanishes. Increasing ϵ enhances the heat transfer, as expected, especially for high values of Rayleigh number.

References

Aydın, O., Ünal, A. and Ayhan, T. (1999a), "Natural convection in rectangular enclosures heated from one side and cooled from the ceiling", *Int. J. Heat Mass Trans.*, Vol. 42, pp. 2345-55.

Aydın, O., Ünal, A. and Ayhan, T. (1999b), "A numerical study on buoyancy-driven flow in an inclined enclosure heated and cooled on adjacent walls", *Numer. Heat Trans. A*, Vol. 36, pp. 585-9.

Chao, P.K.-B., Ozoe, H., Churchill, S.W. and Lior, N. (1983), "Laminar natural convection in an inclined rectangular box with lower surface half-heated and half-insulated", *J. Heat Transfer*, Vol. 105, pp. 425-32.

Chu, H.H.-S., Churchill, S.W. and Patterson, C.V.S. (1976), "The effects of heater size, location, aspect ratio, and boundary conditions on two-dimensional, laminar, natural convection channels", *J. Heat Transfer*, Vol. 98, pp. 1194-201.

Chu, T.Y. and Hichox, C.E. (1990), "Thermal convection with large viscosity variation in an enclosure with localized heating", *J. Heat Transfer*, Vol. 112, pp. 388-95.

Ganzorolli, M.M. and Milanez, L.F. (1995), "Natural convection in rectangular enclosures heated from below and symmetrically cooled from the sides", *Int. J. Heat Mass Trans.*, Vol. 38 No. 6, pp. 1063-73.

Hasnaoui, M., Bilgen, E. and Vasseour, P. (1992), "Natural convection heat transfer in rectangular cavities partially heated from below", *J. Thermophysics Heat Trans.*, Vol. 6 No. 2, pp. 255-64.

Incropera, F.P. (1988), "Convection heat transfer in electronic equipment cooling", *J. Heat Transfer*, Vol. 110 No. 4, pp. 1097-111.

Kamotani, Y., Wang, L.W. and Ostrach, S. (1983), "Natural convection heat transfer in a water layer with localized heating from below", in *Natural Convection in Enclosures HTD*, Vol. 26, pp. 43-8.

Keyhani, M., Prasad, V., Shen, R. and Wong, T.-T. (1988), "Free convection heat transfer from discrete heat sources in a vertical cavity", in *Natural and Mixed Convection in Electronic Equipment Cooling HTD*, Vol. 100, pp. 13-24.

Kim, S.J. and Lee, S.W. (1996), *Air Cooling Technology for Electronic Equipment*, CRC Press, Boca Raton, LA.

November, M. and Nansteel, M.W. (1987), "Natural convection in rectangular enclosures heated from below and cooled along one side", *Int. J. Heat Mass Trans.*, Vol. 30 No. 11, pp. 2433-40.

Patankar, S.V. (1980), *Numerical Heat Transfer and Fluid Flow*, Hemisphere, Washington, DC.

Peterson, G.P. and Ortega, A. (1990), "Thermal control of electronic equipment and devices", *Adv. Heat Transfer*, Vol. 20, pp. 181-214.

Ramos, R.A.V. and Milanez, L.F. (1998), "Numerical and experimental analysis of natural convection in a cavity heated from below", *Proc. 11th IHTC*, Kyongju, Korea, Vol. 3.

Roache, P.J. (1982), *Computational Fluid Dynamics*, Hermosa, Albuquerque, NM.

Torrance, K.E., Orloff, L. and Rockett, J.A. (1969), "Experiments on natural convection in enclosures with localized heating from below", *J. Fluid Mech.*, Vol. 36, pp. 21-31.

Torrance, K.E. and Rockett, J.A. (1969), "Numerical study of natural convection in an enclosure with localized heating from below", *J. Fluid Mech.*, Vol. 36, pp. 33-54.

Turner, B.L. and Flack, R.D. (1980), "The experimental measurement of natural convective heat transfer in rectangular enclosures with concentrated energy sources", *J. Heat Transfer*, Vol. 102, pp. 236-41.

Valencia, A. and Frederick, R.L. (1989), "Heat transfer in square cavities with partially active vertical walls", *Int. J. Heat Mass Trans.*, Vol. 32 No. 8, pp. 1567-74.